Stem Cell Reports
Article

ISSCR

OPEN ACCESS

Identification of a Proximal Progenitor Population from Murine Fetal Lungs with Clonogenic and Multilineage Differentiation Potential

Mélanie Bilodeau,[1] Sharareh Shojaie,[2,3] Cameron Ackerley,[2,4] Martin Post,[2,3] and Janet Rossant[1,5,*]
[1]Program in Developmental and Stem Cell Biology, Peter Gilgan Centre for Research and Learning, The Hospital for Sick Children, Toronto ON M5G 0A4, Canada
[2]Program in Physiology and Experimental Medicine, Peter Gilgan Centre for Research and Learning, The Hospital for Sick Children, Toronto ON M5G 0A4, Canada
[3]Department of Physiology, University of Toronto, Toronto ON M5S 1A8, Canada
[4]Department of Paediatric Laboratory Medicine, The Hospital for Sick Children, Toronto ON M5G 1X8, Canada
[5]Department of Molecular Genetics, University of Toronto, Toronto ON M5S 1A8, Canada
*Correspondence: janet.rossant@sickkids.ca
http://dx.doi.org/10.1016/j.stemcr.2014.07.010

SUMMARY

Lung development-associated diseases are major causes of morbidity and lethality in preterm infants and children. Access to the lung progenitor/stem cell populations controlling pulmonary development during embryogenesis and early postnatal years is essential to understand the molecular basis of such diseases. Using a *Nkx2-1*^{mCherry} reporter mouse, we have identified and captured *Nkx2-1*-expressing lung progenitor cells from the proximal lung epithelium during fetal development. These cells formed clonal spheres in semisolid culture that could be maintained in vitro and demonstrated self-renewal and expansion capabilities over multiple passages. In-vitro-derived *Nkx2-1*-expressing clonal spheres differentiated into a polarized epithelium comprised of multiple cell lineages, including basal and secretory cells, that could repopulate decellularized lung scaffolds. *Nkx2-1* expression thus defines a fetal lung epithelial progenitor cell population that can be used as a model system to study pulmonary development and associated pediatric diseases.

INTRODUCTION

The primitive trachea and two distal lung buds emerge from the anterior foregut endoderm around embryonic day 9.5 (E9.5) (Kimura and Deutsch, 2007). Already at stage E10.5, the trachea comprises epithelial cells expressing the basal cell marker P63, and they increase in number until stage E15.5 (Que et al., 2007, 2009). Branching morphogenesis, characterized by SOX9 expression in the distal lung epithelium, gives rise to the conducting airway and the gas exchange regions throughout the prenatal period (Alanis et al., 2014). Before E15.0, the proximal branches downregulate SOX9, activate SOX2, and undergo conducting airway differentiation (ending at E17.0) (Alanis et al., 2014). ASCL1-expressing neuroendocrine cells become detectable at E12.5 (Li and Linnoila, 2012). The ciliated (*Foxj1*$^+$, β-tubulin$^+$) and club cell (SCGB1A1$^+$) markers are expressed around E14.5–E16.5 (Rawlins et al., 2007, 2009b). In addition, the heterogeneous club cell population expresses early markers (*Scgb3a2*, *Cyp2f2*, and others) and region-specific transcripts (*Reg3g*, *Gabrp*, *Hp*, *Upk3a*, and others) (Guha et al., 2014). After the specification of the bronchioalveolar duct junctions at stage E17.0, alveolar type 1 (AT1) and 2 (AT2) cells differentiate during the sacculation process and mature into functional alveoli in the distal lung (Alanis et al., 2014; Desai et al., 2014; Treutlein et al., 2014). Branching morphogenesis and alveolar differentiation are oppositely regulated by KRAS, SOX9, and others (Chang et al., 2013). Mature basal cells are found postnatally (P63$^+$, KRT14$^+$, KRT5$^+$, BS-I-B4$^+$) (Daniely et al., 2004). Shortly after birth, submucosal glands emerge underneath the proximal airway epithelium, with acini comprised of secretory cells (e.g., mucous and serous cells) and myoepithelial basal cells connected to the surface by ducts made up of basal and ciliated cells (Wansleeben et al., 2013, 2014). The submucosal glands share expression of several markers with surface epithelium (e.g., P63, KRT5, MUC5AC, LTF, and others) but distinctively comprise P63$^+$ KRT5$^+$ SMA$^+$ myoepithelial basal cells (Wansleeben et al., 2014).

In the adult mouse and human lungs, distinct region-specific epithelial progenitor cells have been described (Wansleeben et al., 2013), but their fetal counterparts remain undercharacterized. At E10.5–E12.5, *Id2*-expressing distal tip cells of the fetal lung buds are multipotent and contribute to the conducting airways (e.g., club, ciliated, neuroendocrine) and alveolar (AT1 and AT2) lineages (Rawlins et al., 2009a). Later at stage E15.0, AT1 and AT2 cells derive from a bipotent progenitor (Desai et al., 2014). Inducible lineage tracing regulated by the *Cgrp* promoter (neuroendocrine cell marker) at E12.5–E14.5 labels neuroendocrine and alveolar (AT1 and AT2 cells) descendants (Song et al., 2012). However, *Ascl1*-expressing cells are reported to give rise to airway, AT2, and nonepithelial cells, a finding to be clarified by clonal analysis (Li and Linnoila, 2012). Also, secretory cells contribute to club and ciliated lineages postnatally (Guha et al., 2012). Although these studies reveal the origin of intrapulmonary airways and

alveoli lineages (i.e., distal lung), the progenitor relationships in the proximal trachea and extrapulmonary bronchi (i.e., proximal lung) remain mostly unresolved. Inducible lineage tracing driven by the human *SPC* promoter suggests a distinct origin for proximal and distal lungs (Perl et al., 2002). Moreover, fetal human tracheal tissue can mature into basal, mucociliary, and submucosal gland cells after serial xenotransplantation, suggesting progenitor/stem cell activity (Delplanque et al., 2000).

To better understand lineage relationships in fetal lung development, we knocked an mCherry reporter gene into the *Nkx2-1* locus to isolate purified primary lung epithelial cells that we submitted to in vitro clonogenic progenitor assays. NKX2-1 is the earliest marker of pulmonary fate and is broadly expressed in the proximal and distal fetal lung epithelium (Kimura and Deutsch, 2007). *Nkx2-1*-deficient mice are stillborn and show severe distal lung epithelium branching and cytodifferentiation defects (Kimura et al., 1996; Minoo et al., 1999). Also, their trachea epithelium fails to separate from the esophagus and adopts an esophagus-like phenotype, with high expression of SOX2 and P63 (Minoo et al., 1999; Que et al., 2007). Our molecular characterization of *Nkx2-1*-expressing cells reveals an underappreciated broad cellular diversity in the airways, including progenitor cells with long-term clonogenic and differentiation potential in vitro. These cells self-renew and engraft when seeded onto decellularized lung scaffolds. Overall, these results suggest that the *Nkx2-1*-expressing population in the fetal proximal airways contains cells that can act as self-renewing multilineage progenitors in vitro.

RESULTS

In Vitro Colony-Forming Potential of *Nkx2-1*-Expressing Cells

To capture mouse pulmonary cells expressing *Nkx2-1*, a nondisruptive fluorescent mCherry knockin allele was generated by gene targeting in embryonic stem cells (ESCs) (Figure 1A; Figure S1A available online). Both heterozygous and homozygous animals generated were normal and fertile and could be used for experiments. mCherry was detected by fluorescent microscopy in *Nkx2-1*-expressing tissues: the lung, brain, and thyroid (Figures 1B and S1B) (Lazzaro et al., 1991). At the cellular level, confocal imaging revealed coexpression of cytoplasmic mCherry and immunostained nuclear NKX2-1 in fetal and adult lungs (Figures 1C and S1C). The percentage of *Nkx2-1*-mCherry-positive (mC$^+$) cells varied from 9% to 20% in total lung tissue isolated from E10.5 to E15.5 (Figures S1D and S1E). To better understand the cell diversity expressing *Nkx2-1* in the developing lung (E11.5–E15.5), pan-epithelial and lineage-specific markers were monitored by quantitative real-time PCR in *Nkx2-1*-mC$^+$ and *Nkx2-1*-mCherry-negative (mC$^-$) sorted cells and by coimmunostaining at fetal and adult stages (Figures S1F and S2A–S2J; data not shown). NKX2-1 was expressed in most of the specialized airway cells (basal, club, and ciliated), in the tracheal submucosal glands, and in distal AT2 cells (Figures S2A–S2J). Therefore, NKX2-1 expression is not restricted to club or AT2 cells, as generally assumed (Kimura and Deutsch, 2007).

To assess whether *Nkx2-1*-expressing cells have progenitor activity, an in vitro colony assay was optimized. The stage E14.5 was initially selected for two reasons: (1) the amount of material available and (2) the expression profile of lineage-specific markers suggested that cytodifferentiation started around this time (data not shown). Proximal and distal lung epithelial cells were separately sorted based on *Nkx2-1*-mCherry expression and embedded in a Matrigel-based semisolid medium supplemented with growth factors, without supporting cells (Figures 1D and 1E). Morphologically distinct colonies were derived at a higher frequency in the mC$^+$ fraction in contrast to the mC$^-$ fraction (52-fold or 99-fold enrichment of mC$^+$ over mC$^-$ colonies, from proximal or distal lung regions, respectively; Figures 1E and 1F). Colonies derived from the proximal epithelium had compact or spheroid shapes of various sizes with cells tightly connected together (Figure 1E). Colonies derived from the distal lung epithelium were small with irregular morphologies (Figure 1E). Within the context of the provided culture conditions, only the colonies derived from the proximal lung could be propagated in long-term culture (e.g., >150 days, 15 passages [p.15]), as illustrated by cell numbers at first passage postsorting (Figure 1G). Quantitative real-time PCR was used to assess gene expression in pooled populations of 12- to 13-day-old colonies from the second passage (Figure 1H). Colonies derived from both the proximal and distal lung expressed *Nkx2-1*, *Scgb3a2*, *Scgb1a1*, *Muc5ac*, *Id2*, *Pdpn*, *Aqp5*, and *Ltf* (Figure 1H). However, expression of basal and ciliated cell markers (e.g., *Trp63*, *Krt5*, and *Foxj1*) and the distal lung/AT2 cell marker *Sftpc* was restricted to colonies derived from the proximal or the distal lung, respectively (Figure 1H). Expression of several cell markers was higher in cultured cells than in freshly sorted E14.5 mC$^+$ parental cells, a feature more reminiscent of later developmental stages (Figure 1H). The neuroendocrine (*Ascl1*) cell marker was expressed at low level in both colony types (Figure 1H). Overall, at E14.5, the *Nkx2-1*-expressing cells gave rise to colonies with distinct characteristics depending on their region of origin. We focused on the characterization of the putative progenitor cells derived from the fetal upper airways because of their relevance for several pediatric diseases, including cystic fibrosis, asthma, and others.

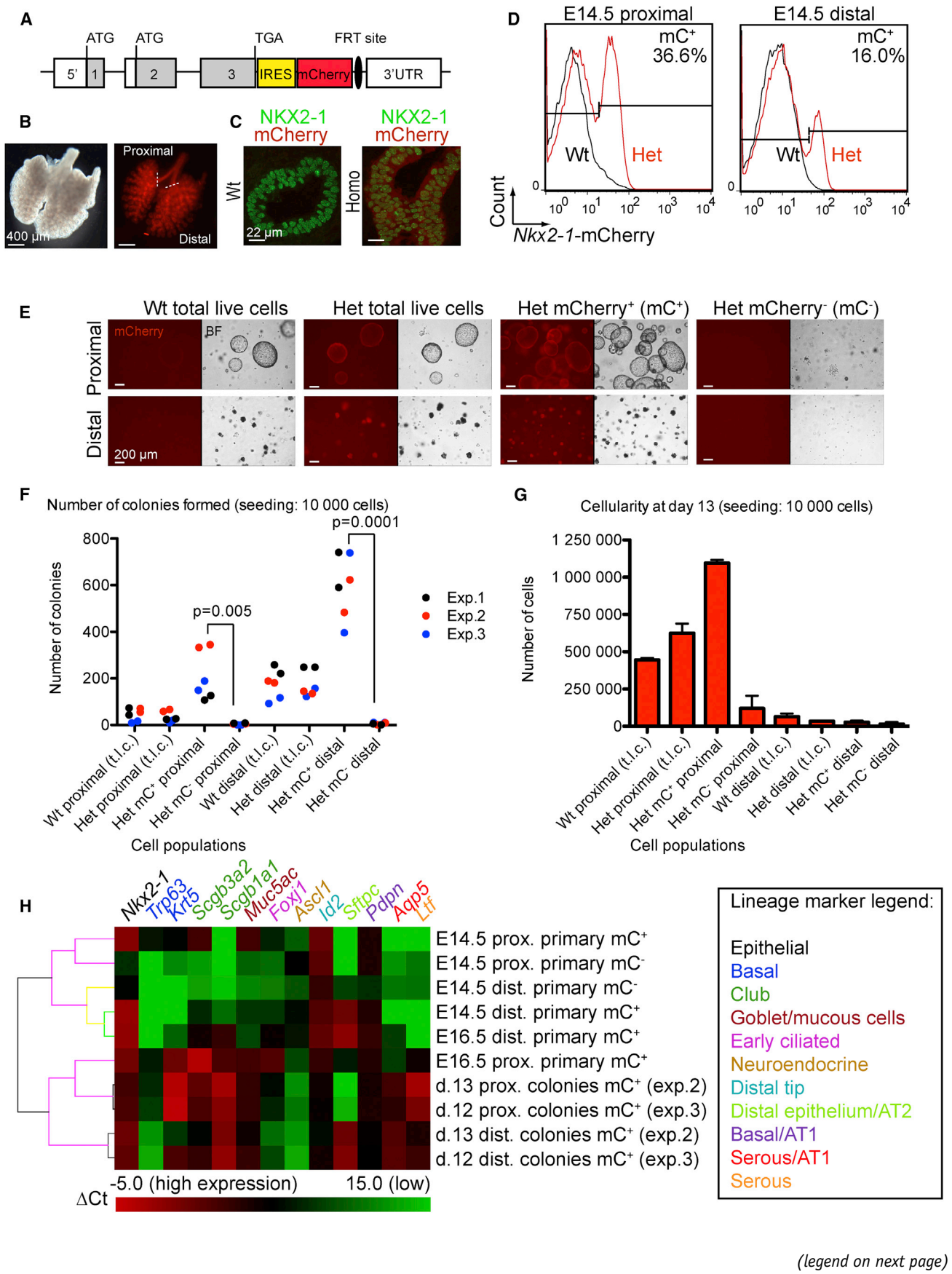

(legend on next page)

Colony Propagation

Media formulation to derive colonies was based on published protocols developed for maintaining primary pulmonary cells/tissues and included fetal bovine serum (FBS), insulin, modulators of membrane transporters or cyclic AMP-dependent pathways (forskolin and 3-isobutyl-1-methylxanthine), epidermal growth factor (EGF), hepatocyte growth factor (HGF), and fibroblast growth factors (FGFs) 1, 7, and 10 (Figure S3A) (McQualter et al., 2010; Shannon et al., 1999). Media components were individually removed to assess their requirements on colony number, cellularity, and gene expression (Figures S3A–S3L). Overall, removal of any media component, except the FGFs, altered the tested parameters (Figures S3A–S3L). Of note, basal, early ciliated, and mucosecretory cell phenotypes were differently altered according to the culture conditions (Figures S3D–S3L). Removal of FGFs, in presence of all other components, caused minimal effect, and colonies continued to proliferate (data not shown).

To understand the sequential molecular changes occurring during colony propagation, expression analyses by quantitative real-time PCR for selected gene markers were conducted over a 12-day time course for two independent populations of mC^+ colonies (p.7 and p.15) (Figures S4A–S4H). Overall, these results suggested that in established cultures, basal and early secretory cells were stably present throughout colony formation (days 2–12), whereas club and mucociliary cells developed progressively between each passage (day 6 and after) (Figures S4A–S4H). In addition, cells from each polyclonal population expressed receptors for EGF, HGF, and insulin (Figure S4C).

Comparison of In Vitro Progenitor Activity at E12.5 and E14.5

Next, cell sorting was conducted at an earlier stage (i.e., E12.5) to determine whether progenitors with in vitro potential could be detected prior to E14.5 when the epithelium is less differentiated. Spheroid colonies could be derived from the proximal region more efficiently at E12.5 than at stage E14.5 (Figures 2A and 2B). E12.5-isolated distal *Nkx2-1*-expressing cells gave rise to saccular colonies similar to E14.5-derived samples but with reduced frequency (Figures 2A and 2B). Immunostaining of proximal polyclonal colonies isolated at stages E12.5 and E14.5 revealed expression of NKX2-1, P63, and SCGB1A1 in both groups (Figure 2C). Individual E12.5 and E14.5 proximal colonies were isolated at day 20 (p.2) to evaluate their common or unique expression characteristics by quantitative real-time PCR (Figure 2D). At E12.5, parental primary mC^+ cells showed an absence or low levels of most lineage markers tested except *Nkx2-1*, *Sox2*, and *Krt8* (Figure 2D). At E14.5, parental primary cells expressed higher levels of *Trp63*, *Krt5*, *Scgb3a2*, *Cyp2f2*, *Muc5ac*, and low levels of other markers (Figure 2D). Colonies derived from E12.5 stage generally expressed higher levels of *Sox2*, *Trp63*, *Krt5*, and *Ascl*1 (Figure 2D). Colonies derived from E14.5 stage generally expressed higher levels of *Krt8*, *Reg3g*, *Upk3a*, and *Foxj1* (Figure 2D). No differences were observed for *Nkx2-1*, *Scgb1a1*, *Scgb3a2*, *Cyp2f2*, *Gabrp*, *Muc5b*, *Muc5ac*, *Ltf*, and *Aqp*5 (Figure 2D). In fact, the gene expression profile of one E12.5-derived colony (i.e., D12) clustered with the E14.5-derived colonies (Figure 2D). The differentiation level of E12.5–E14.5 proximal lungs was also verified by immunostaining (Figures 2E–2H). At stage E12.5 compared to E14.5, fewer epithelial cells expressed P63 (average frequency of 0.202 ± 0.139 at E12.5 and 0.563 ± 0.100 at E14.5; two-tailed Student's t test, $p = 0.00003$, Figure 2E). FOXJ1 and MUC5AC proteins were weakly detected at stage E14.5, but not at stage E12.5 (Figures 2F and 2G). The club cell marker SCGB1A1 was not expressed yet at stage E14.5 (Figure 2H). Overall, spheroid colonies were efficiently derived from the poorly differentiated proximal lung epithelium at stage E12.5. Once established, colonies derived from stage E12.5 had higher expression of basal and neuroendocrine cell markers compared to colonies derived from stage E14.5. Colonies

Figure 1. Colony-Formation Assay with E14.5 Proximal and Distal Lung Cells

(A) mCherry knockin in the *Nkx2-1* locus. Gray boxes indicate exons 1–3. UTR is shown in the open box. ATG or TGA indicates translation initiation or termination codon.

(B) mCherry fluorescence detected by microscopy in the lungs of an E13.5 *Nkx2-1*^{mCherry} mouse.

(C) Cryosection immunostaining showing nuclear NKX2-1 correlating with cytoplasmic mCherry expression in the lung epithelium of an E13.5 homozygous (homo) *Nkx2-1*^{mCherry} mouse.

(D) Representative flow cytometry profiles of pulmonary cells harvested from WT or heterozygote (het) *Nkx2-1*^{mCherry} mice.

(E) Twelve-day-old colonies derived from sorted cell populations (p.1). BF, bright field.

(F) Number of colonies observed for the indicated populations (scoring between days 6 and 12). Three independent experiments (Exp.) were performed in duplicate (dots). Significance was determined with a two-tailed Student's t test (p value). t.l.c., total live cells.

(G) Cellularity monitored at p.2 for a selected experiment. Values represent average of duplicate samples with SD.

(H) Gene expression of selected markers monitored by quantitative real-time PCR in the indicated primary sorted cells or polyclonal colony populations. Values are normalized to the average of *Actb* and *Hprt1* genes (ΔCt). ΔCt >15 may represent low or no expression. prox., proximal; dist., distal.

See also Figures S1–S4 and Tables S2 and S3.

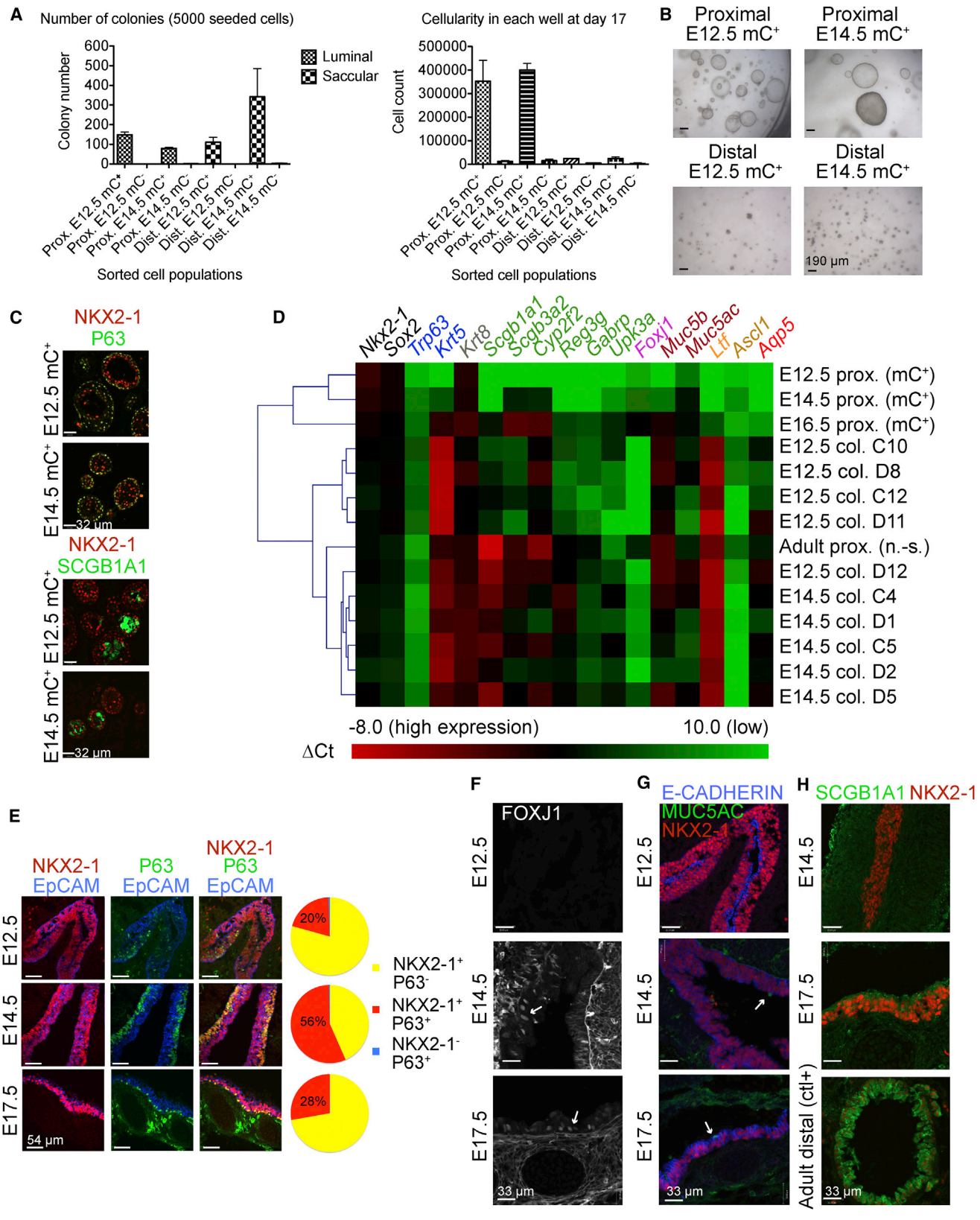

(legend on next page)

derived from stage E14.5 expressed higher levels of selected club cell markers and early ciliated cells. Expression levels of several mucosecretory markers were similar for both groups.

Fractionation of Primary Cells with ITGB4

To get a better understanding of the colony-initiating cells, we aimed to use a cell surface marker to further fractionate mC$^+$ cells by flow cytometry. First, we did a developmental time course of basal cell maturation in mouse proximal airways using immunostaining with a panel of known markers, including cell surface markers (Figure S5A) (Rock et al., 2009; Wansleeben et al., 2013). P63 was already detectable at stage E10.5 (Figure S5A). Up to stage E14.5, the markers of mature basal cells (i.e., PDPN, KRT5, ITGA6, and NGFR) were either not expressed or not restricted to P63-expressing cells (Figures S5A and S5B). P63-expressing cells coexpressed KRT5, PDPN, and ITGA6 at E16.5 and NGFR postnatally (Figure S5A). Therefore, at stages E12.5–E14.5, P63-expressing cells may be considered as prebasal as suggested before (Daniely et al., 2004), and classical basal cell surface markers are not useful to fractionate the epithelium.

ITGB4 came to our attention as a candidate proximal cell surface marker following region-specific microarray analyses of fetal cells (M.B. and J.R., unpublished data). ITGB4 was previously shown to be a marker of adult basal cells (Delplanque et al., 2000). Immunostaining of E14.5 wild-type (WT) lungs revealed ITGB4 expression in the trachea and conducting airways, but not in the distal acinar tubules and buds (Figure S5C). ITGB4 was enriched at the basolateral side of tracheal cells attached to the basement membrane (Figure S5C). Using flow cytometry, a range of ITGB4 expression was detected in proximal mC$^+$ cells allowing segregation according to high or low expression level (i.e., ITGB4^{+Hi} or ITGB4^{+Lo}, respectively) (Figure S5D). According to quantitative real-time PCR analysis, this fractionation method significantly enriched prebasal cells expressing *Krt5* mRNA into the mC$^+$ITGB4^{Hi} fraction ($p = 0.018$), without segregating most mucosecretory cells (Figure S5E). Functionally, the morphology, expression profile, and frequency of spheroid colonies were similar with both sorted cell fractions (Figures S5F and S5G; data not shown). Overall, these data suggested that at stage E14.5, the colony-forming ability did not correlate with the expression levels of ITGB4 or basal cell markers.

Clonogenicity of Colonies Derived from Stage E14.5

To determine whether proximal colonies were derived from single cells or from aggregation/migration events, a cell-mixing experiment was performed with sorted mC$^+$ cells and EpCAM$^+$-stained cells from mice expressing EGFP ubiquitously (Figure 3A). EpCAM is a marker of epithelial cells that can also separate fetal lung epithelium from surrounding mesenchyme. The frequency of colony formation was similar for both mC$^+$ and EpCAM$^+$ populations sorted individually, suggesting that this ability is similarly located within both cell compartments at E14.5 (Figure 3B). When both differentially labeled cell populations were mixed together, most colonies were monochromatic mC$^+$ or EGFP$^+$ as monitored with fluorescence microscopy, suggesting a clonal origin (Figures 3C and 3D). Individual colonies were confirmed to share similar gene expression profiles by quantitative real-time PCR (data not shown).

Immunofluorescence of colonies (14–22 days old) derived from mC$^+$ cells confirmed their multicellularity, implying proliferation of the initial single cells (Figures 3E–3I). Staining of colonies with NKX2-1 showed widespread cellular expression, but only a fraction of the cells expressed P63 (Figure 3E). Some colonies expressed MUC5AC, whereas SCGB3A2 expression was more widespread (Figure 3F). In addition, some NKX2-1$^+$ cells expressed SCGB1A1, FOXJ1, and AQP5 (Figures 3G and 3H). Myoepithelial basal cells expressing KRT5 and SMA could be detected in some colonies, suggesting a submucosal gland phenotype (Figure 3I). Overall, the mC$^+$ cells produce clonal colonies able to proliferate and differentiate, demonstrating progenitor activity.

Clonal Self-Renewal of Colonies

To assess self-renewal capacity, serial passaging of primary (parental) and secondary (daughter) colonies was performed to obtain tertiary (granddaughter) colonies

Figure 2. Colony Formation of E12.5 and E14.5 Primary Cells

(A) Colony-formation assay with *Nkx2-1*-mC$^+$ or *Nkx2-1*-mC$^-$ cells sorted from proximal (Prox.) or distal (Dist.) lung regions at E12.5 or E14.5. The left panel shows the colony number from two experiments performed in duplicate (average and SD). The right panel shows the cellularity for experiment number 1 (average from two wells with SD).

(B) Images of colonies at 17 days (p.1).

(C) Immunostaining of mC$^+$ colonies derived at E12.5 and E14.5 (16 days old, p.6).

(D) Quantitative real-time PCR performed with RNA extracted from individual day 20 (p.2) mC$^+$ colonies (col.) or primary sorted (mC$^+$) or nonsorted (n.-s.) cells (n = 1 experiment). ΔCt heatmap with normalization of Ct values of indicated target genes to average of *Actb* and *Hprt1* genes. The cutoff was set to a ΔCt of 10 (Ct 25–34 for reference genes). For the lineage marker legend, refer to Figure 1H.

(E–H) Immunostaining of proximal lung epithelial cells from WT mice. Ctl$^+$, positive control.

See also Figure S5 for fractionation of proximal cells and Tables S2 and S3.

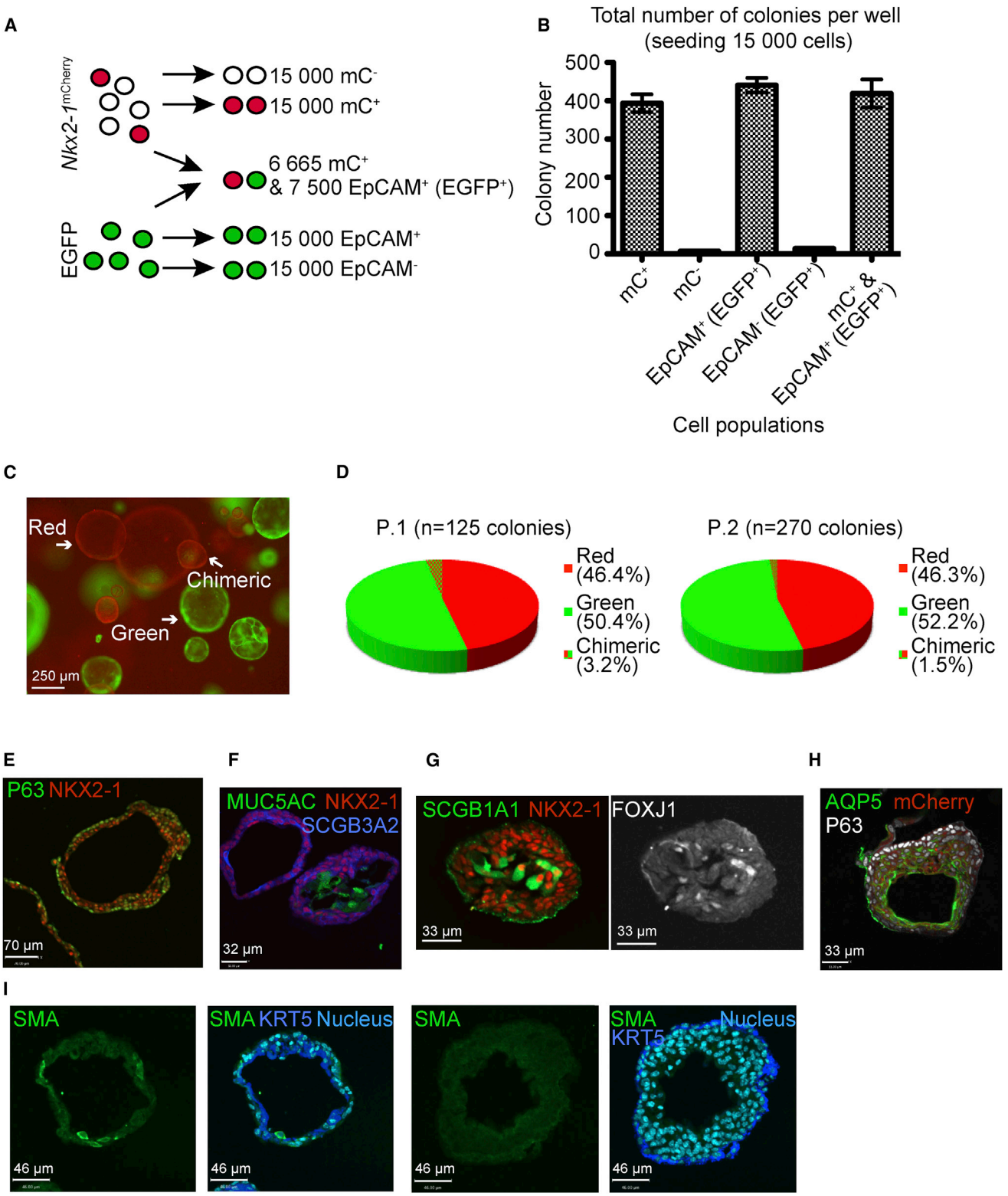

Figure 3. Clonogenicity and Differentiation of the Colonies Derived from E14.5 Proximal Lungs

(A) Cell-mixing experiment performed with colonies derived from proximal lungs of E14.5 *Nkx2-1*^{mCherry} or B5/EGFP mice (mCherry and EpCAM cell sorting, respectively). mC, mCherry.

(legend continued on next page)

(Figure 4A). When 16- or 20-day-old primary colonies from E12.5 or E14.5 were isolated and tested for their ability to give rise to secondary colonies, their clonogenic potential varied (i.e., 0–1,372 secondary colonies) (Figure 4B). Of 53 tested colonies, 8 (15%) did not give rise to secondary colonies (Figure 4B). The clonogenic capacity did not correlate with the diameter of the primary colonies (Pearson correlation coefficient, 0.26; Figure 4B). During serial passaging of 14 different series of primary and secondary colonies derived from mC^+ cells at stage E12.5 or E14.5 or WT E14.5 cells, most secondary colonies tested gave rise to at least two tertiary colonies (n = 61 out of 76 secondary colonies tested, i.e., 80%). The number of tertiary colonies derived from secondary colonies ranged from 0 to 693, suggesting functional heterogeneity at the cellular level in parental colonies (Figures 4C and 4D). Overall, the self-renewal capacity of cells present in most series led to expansion of the primary colony through two serial passages (Figures 4C and 4D). Histological analyses confirmed similar morphology and expression in two selected clonal culture series (Figure 4E).

To further evaluate the expression characteristics and heterogeneity, RNA was extracted from individual serial colonies derived from E12.5 mC^+ primary cells at the time of passaging (Figures 5A–5C). Expression profiling by quantitative real-time PCR of individual colonies from three independent series revealed that most of them show common gene expression (e.g., *Nkx2-1*, *Sox2*, *Krt5*, *Ltf*, etc.), but expression of other genes varied (Figure 5D). For example, in the series initiated with the primary colony 2-D5, two secondary and three tertiary colonies shared a similar expression pattern of *Scgb3a2*, *Scgb1a1*, and other gene markers (Figure 5D). However, one of the tertiary colonies (i.e., 2-D5-3-2) did not express *Ltf* (Figure 5D). Also, the expression profile of primary colonies 2-D7 and 2-E1 was similar to 2-D5, although with higher levels of *Muc5ac* (Figure 5D). Each of these gave rise to one secondary colony expressing a low level of both *Scgb3a2* and *Scgb1a1* (i.e., 2-D7-1 and 2-E1-1, respectively) and one expressing a higher level of single or both *Scgb3a2* and *Scgb1a1* (i.e., 2-D7-3 and 2-E1-2, respectively) (Figure 5D). These expression patterns were conserved in their daughter-tertiary colonies (Figure 5D). Overall, these results suggest that a subset of primary cells derived from fetal proximal lungs can self-renew and expand in culture and give rise to serial colonies, which preserve similar expression characteristics. All colonies tested showed expression of two or more conducting airway-lineage markers, suggesting that the colony-initiating cells are multipotent progenitors. However, cellular heterogeneity is also created among colonies, and the ability to give rise to daughter colonies and/or the differentiation potential may vary. Therefore, the multipotent progenitor cells are functionally heterogeneous.

Multilineage Differentiation Potential of Fetal Primary Cells and Clonal Progenitor Colonies

To further characterize the differentiation potential of fetal primary and cultured cells, a repopulation assay of decellularized lung scaffolds was employed. Decellularized adult rat lung scaffold cultures were maintained for 2–3 weeks at the air-liquid interface in a defined, serum-free basal media. First, the potential of E12.5 and E14.5 freshly sorted primary cells (i.e., mC^+ or mC^- cells) was tested (see Figure S6A for initial gene expression). Culture of E14.5 proximal mC^+ primary cells on scaffolds led to the formation of an epithelium constituted of cells expressing markers of basal, club, and ciliated cells, reminiscent of native tracheal epithelium (Figure 6A; Table S1). Transmission and scanning electron microscopy (TEM and SEM, respectively) revealed a polarized epithelium (i.e., apical microvilli, junctional complexes, and basement membrane) with cells of various morphologies (stages E12.5 and E14.5: Figures 6B and S7A; Table S1). This included ciliated cells and glycogen-abundant secretory cells, characteristic of embryonic and postnatal respiratory epithelium (El-Gawad and Westfall, 2000; Massaro et al., 1984). The E12.5 and E14.5 distal mC^+ primary cells also gave rise, but less efficiently, to a polarized epithelium comprised of cells with club, ciliated, and basal cell characteristics (Figures S6B and S6C; Table S1; data not shown). Under these conditions, expression of SFTPC (i.e., early distal epithelium and/or AT2 cells) was detected at low levels in scaffolds seeded with distal primary cells, whereas it was absent with seeded proximal cells (Figures 6A and S6B; Table S1). Also, PDPN-expressing cells that were negative for P63 (i.e., AT1 cells) were sparse or absent (Figures 6A and S6B; Table S1). In fact, most primary cells repopulating the scaffolds, either derived from proximal or distal lung regions, expressed SOX2, suggesting that an airway phenotype predominated (Figures 6A and S6B; Table S1). Decellularized scaffolds were comprised mainly of distal lung regions with some areas of main stem bronchi. Both regions of scaffolds repopulated and

(B) Total colony number for each well (average and SD of duplicate wells; n = 1 experiment).
(C) Representative colonies at day 12.
(D) Scoring of colonies (8–12 days old) based on fluorescence at p.1 and p.2 in three independent wells.
(E–I) Immunostaining with indicated antibodies of colonies derived from the proximal lung of E14.5 *Nkx2-1*^{mCherry} mice (14–22 days old, p.2–p.6).
See also Table S3.

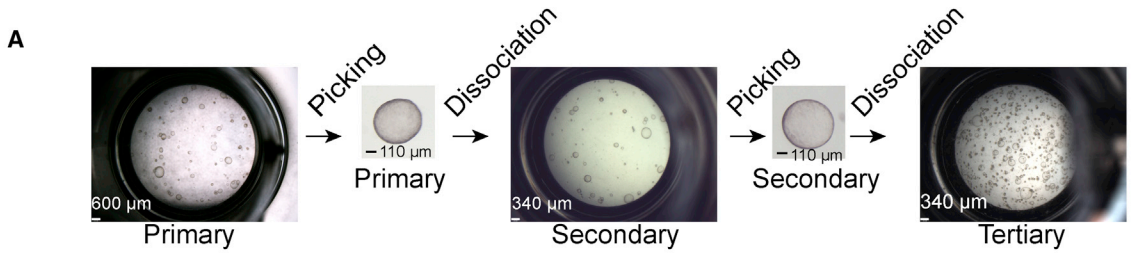

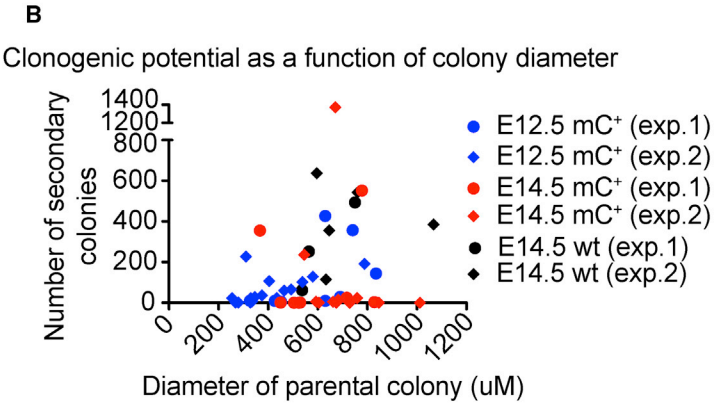

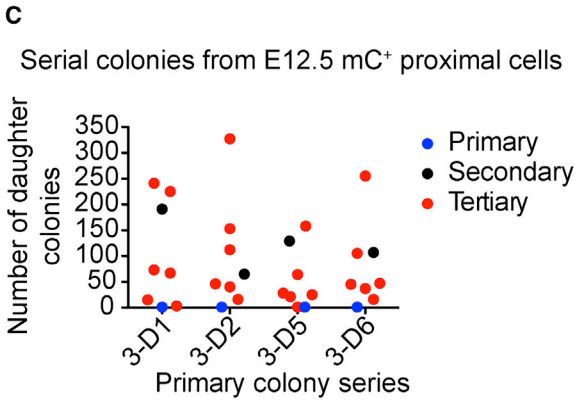

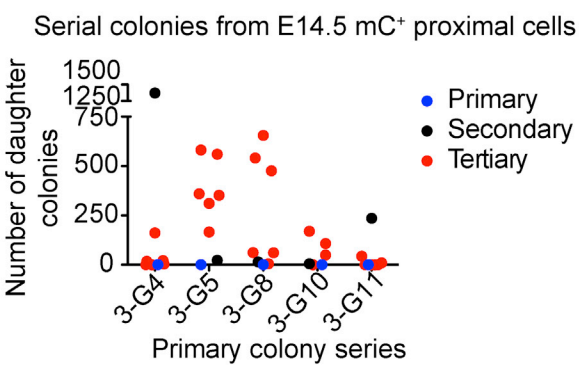

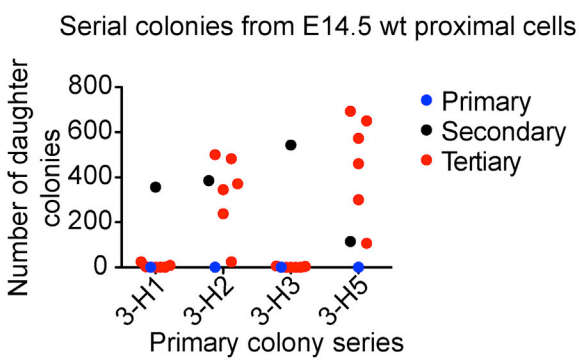

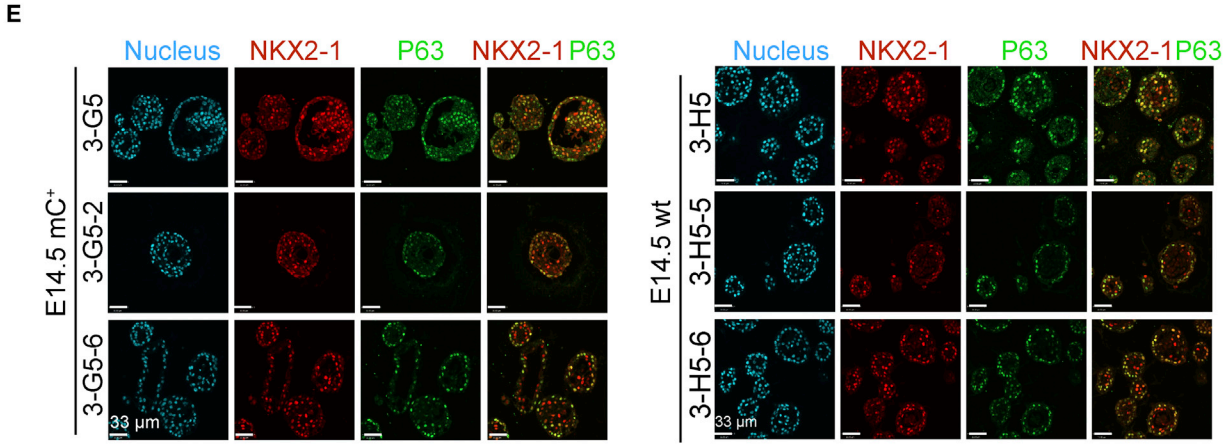

(legend on next page)

promoted similar airway-lineage differentiation. E14.5 proximal or distal mC$^-$ cells repopulated the scaffolds in a scattered matter, with most cells negative for NKX2-1 or other epithelial markers (Figure S6D; Table S1; data not shown).

Next, the potential of polyclonal cultured cells and seven clones was assessed (see Figure S6A for initial gene expression and summary in Table S1). Each of these cultures gave rise to a polarized epithelium comprised of at least two to three distinct proximal cell types characterized by immunostaining and/or electron microscopy (Figures 6C, 7A, 7B, and S7B–S7D; data not shown; summary in Table S1). Basal and secretory cells predominated, and the polyclonal and clonal cultured cells had variable/lower potential to generate ciliated cells (Figures 6C, 7A, 7B, and S7B–S7D; data not shown; Table S1). The engraftment phenotypes of cultured cells were consistent with quantitative real-time PCR and immunostaining analysis of the spheres (Figures 2C, 3E–3H, 4E, 5D, and S6A). Aside from airway surface epithelial markers, immunostaining analyses suggested the presence of myoepithelial basal cells in the colonies (Figure 3I). In agreement with these results, SEM imaging revealed the presence of pits reminiscent of the formation of submucosal glands in the clonal cultures (Figure 7B) (Smolich et al., 1978). As expected, expression of NKX2-1 or mCherry was associated with all cell types repopulating the scaffolds (Figures 6A, 6C, 7A, S6B, S7B, and S7C; data not shown). Repopulation with colony cultures led to extensive SOX2 expression and absence of SFTPC expression (Figures 6C, 7A, S7B, and S7C; Table S1; data not shown). Overall, primary and cultured cells isolated from proximal lungs could engraft when seeded onto decellularized lung scaffolds, generating a polarized epithelium comprising at least two different airway cell types.

DISCUSSION

In this study, we demonstrated that a subset of *Nkx2-1*-expressing cells, derived from the mouse fetal proximal airways, has in vitro clonogenic and multilineage differentiation potential toward airway surface epithelium and submucosal gland cells. *Nkx2-1*-expressing cells from E12.5–E14.5 lungs could generate single-cell-derived epithelial spheres that could be propagated and passaged for an extended period of time in culture due to their self-renewal capacity. These spheres contained differentiated cells predominantly expressing markers of basal and secretory lineages, with less efficient generation of ciliated and submucosal gland cells. Our findings are in agreement with published work suggesting that the submucosal glands are derived from the tracheal epithelium postnatally (Engelhardt et al., 1995). Moreover, our data extend the observations that the early lung anlage has the potential to generate both tissues (Péault et al., 1994) and suggest that the tissues arise from clonogenic multipotent progenitors already present in the proximal region at stage E14.5.

An additional feature of our system compared to other in vitro methods to maintain clonal adult proximal progenitors/stem cells (Hegab et al., 2011; Rock et al., 2009) is the enhanced ability to capture precursors that will differentiate into mature secretory club cells. Not only could we readily detect SCGB1A1 expression by immunostaining, but also ultrastructural analysis revealed the presence of cells covered with microvilli and actively producing secretory granules. Moreover, our culture conditions allow the obtainment of a diversity of club cells according to the expression of region-specific markers such as *Reg3g*, *Gabrp*, and *Upk3a* (Guha et al., 2014).

The relationships of the proximal fetal lung progenitor pool characterized in this study to other epithelial cell types remain to be investigated. In the proximal lung of adult animals, either club cells expressing SCGB1A1 or basal cells expressing KRT5, ITGA6, and NGFR (and others) acts as multipotent progenitor/stem cells (Rawlins et al., 2009b; Rock et al., 2009; Tata et al., 2013). However, at the stage of fetal development that we studied (i.e., E12.5–E14.5), the mature cells characterized by these markers are not detectable yet. These early proximal progenitors are also distinct from other populations previously characterized in murine fetal lungs. For example, they functionally differ from early secretory cells expressing *Scgb3a2* and *Upk3a* (Guha et al., 2012) because they give

Figure 4. In Vitro Self-Renewal of Primary Fetal Lung Cells

(A) Serial passaging of colonies to assess in vitro self-renewal.

(B) The capacity of isolated primary colonies to give rise to secondary colonies did not correlate with their sizes. Sixteen- to 20-day-old primary colonies were isolated at p.2–p.3 from two independent experiments (exp.) (sorting day = p.1).

(C and D) Serial passaging of isolated primary and secondary colonies resulted in the formation of tertiary colonies through self-renewal expansion. For colonies derived from stage E12.5 (C) or E14.5 (D), primary colonies were isolated at p.2 or p.3 (16 days old) and secondary colonies at p.3 or p.4 (16 days old), respectively. Each dot represents the number of daughter colonies derived from a unique parental colony. For each clonal series, daughter colonies from four to five primary or from four to six secondary colonies were scored.

(E) Paraffin section immunostaining of primary clones 3-G5 and 3-H5, and two daughter cultures for each (15–17 days old, p.6–p8).

See also Table S3.

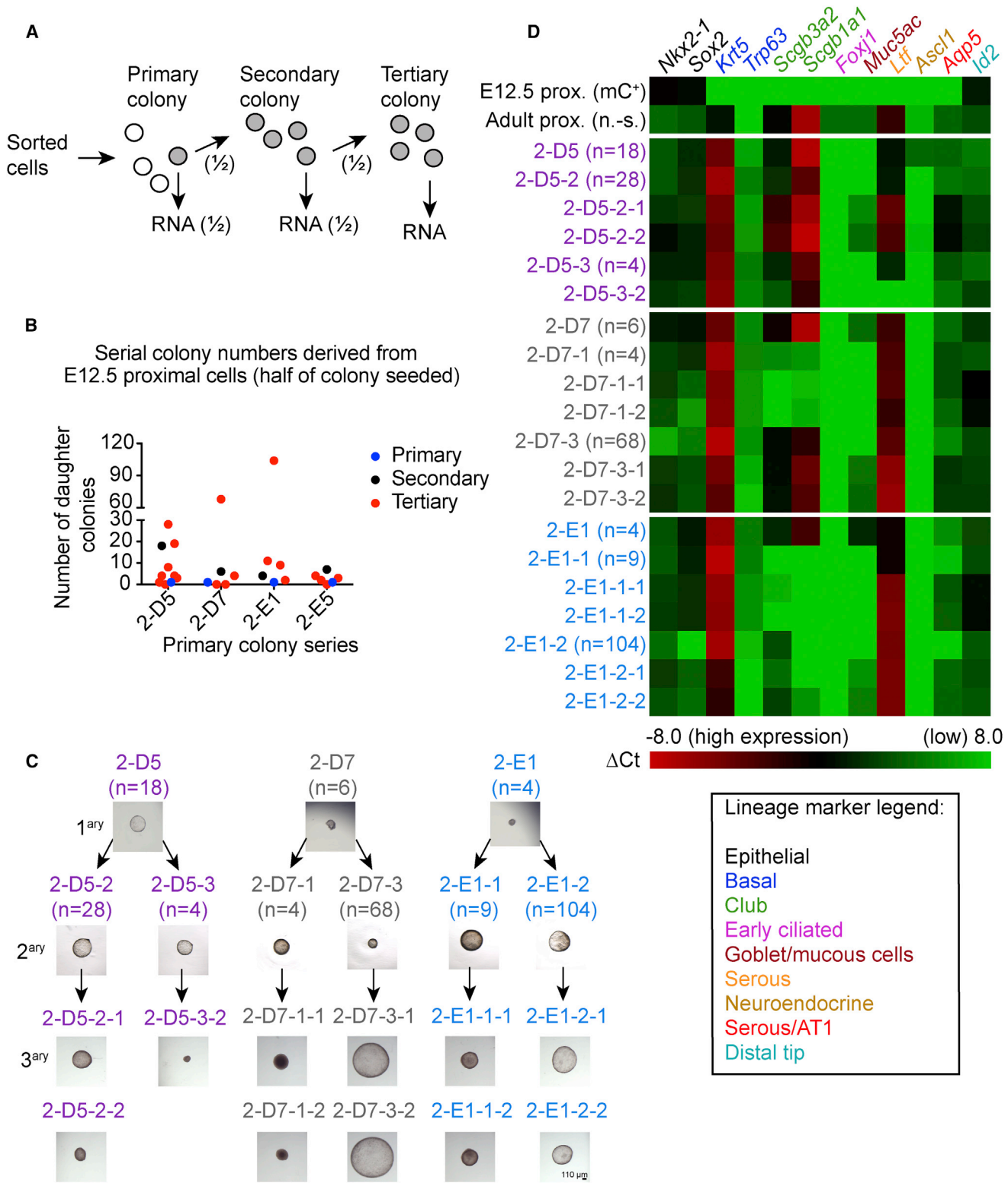

Figure 5. Self-Renewal Assessed with Individual Serial Colonies

(A) In vitro self-renewal assay with serial single colonies and RNA extraction.

(B) Number of secondary colonies derived from half of 18-day-old primary colonies (n = 4 primary colony series, p.1) and number of tertiary colonies derived from half of 23-day-old secondary colonies (n = 4–8 secondary colonies tested per series, p.2).

(legend continued on next page)

rise to basal and submucosal gland cells in addition to club and ciliated cells. Also, their proximal location and lineage contribution differ from the distal multipotent tip cells or bipotent alveolar progenitors (Desai et al., 2014; Rawlins et al., 2009a). Therefore, we believe that our characterization of early proximal lung progenitors extends our knowledge of the cellular mechanisms of fetal pulmonary development.

Postnatal basal cells are multipotent stem cells in the mouse and human upper airways and, perhaps, in the human lower airways where they are also found (Rock et al., 2009). Prebasal cells expressing P63 were found as early as E10.5 in mouse proximal lungs. Fractionation of E14.5 mC^+ cells with ITGB4 revealed that the colony-formation frequency did not correlate with the enrichment of prebasal cells in the $ITGB4^{+Hi}$ fraction. Therefore, our results suggest either that nonbasal epithelial cells adopt a basal-progenitor fate when isolated from other cells, as observed with adult lungs (Tata et al., 2013), or a nonbasal or undifferentiated cell population(s) of the fetal trachea is endowed with in vitro clonogenic self-renewal and differentiation potential. Supporting the latter possibility, a tracheal epithelium comprised of ciliated and other columnar cells does develop in fetal mice lacking basal cells (Daniely et al., 2004), and we efficiently derived more colonies at E12.5 when $P63^+$ cell numbers were lower than at E14.5. Therefore, additional clonal and functional analyses will be required to distinguish whether the progenitor activity is a property of a specific cell subpopulation(s) or whether all early *Nkx2-1*$^+$ cells act as facultative progenitors depending on the environmental context.

Our findings are likely relevant to human biology. In human lungs, basal cells are detectable at gestational age 25 weeks and later ($KRT14^+$) (Broers et al., 1989). Up to gestational age 10 weeks, the lung epithelium comprises unspecialized columnar cells (Broers et al., 1989). Undifferentiated fetal human lung bud tissues or cell suspensions (stage 5–8 weeks) can reconstitute a pseudostratified mucociliary epithelium in vivo in denuded trachea explants (Delplanque et al., 2000). In comparison to our study, 8-week-old fetal human lungs correlate with E12.0 murine lungs (Kimura and Deutsch, 2007). Here, we show that some E12.5 mouse cells isolated from the poorly differentiated proximal airway epithelium are multipotent and self-renewing. Identification of this same progenitor population during differentiation of human pluripotent stem cells to lung cells could provide a renewable resource of lung progenitors for disease modeling and lung repair.

Finally, our *Nkx2-1*^{mCherry} reporter mouse line, phenotypically normal in a homozygous state, is a practical alternative to the *Nkx2-1*^{EGFP} reporter mouse previously reported, which has to be maintained in a heterozygous state because one allele of the gene is disrupted (Longmire et al., 2012). Our mouse line is advantageous for in vivo experiments because heterozygous or homozygous *Nkx2-1* mutations are haploinsufficient or lethal, respectively (Kimura et al., 1996; Pohlenz et al., 2002).

In conclusion, this manuscript describes a progenitor population derived from the fetal proximal lungs that show long-term proliferation in vitro due to their self-renewal capacity. These early cells give rise to basal and secretory cells either inside clonogenic colonies or upon engraftment onto decellularized lung scaffolds. Overall, this study identifies a discrete population of primary fetal proximal airway cells acting as regional progenitor cells that can be maintained, expanded, and used as an in vitro modeling system to study pulmonary development and associated pediatric diseases.

EXPERIMENTAL PROCEDURES

Gene Targeting

The *Nkx2-1* knockin vector comprised an internal ribosomal entry site (IRES) coupled to an mCherry reporter gene (Clontech Laboratories), two homology arms spanning chromosome 12 (57630246–57637428; National Center for Biotechnology Information 37/mm9, 2007), a Flp recombination target-flanked *Pgk*-puro-tk (van der Weyden et al., 2005), and a diphtheria toxin fragment A counterselection cassette. The targeting vector was sequenced, linearized, and electroporated in 10^7 R1 ESCs maintained as described by Nagy et al. (1993). Following puromycin selection (1.5 μg/ml; Sigma-Aldrich), genomic DNA of isolated ESC clones was extracted with DNAzol (Invitrogen). Additional details are described in the Supplemental Experimental Procedures, Figure S1, and Table S2. The *Pgk*-puro-tk cassette was removed by transient expression of a FlpO plasmid (Raymond and Soriano, 2007).

Generation of the *Nkx2-1*^{mCherry} Mouse Line

Two targeted ESC clones (i.e., F4-6 and H1-2), confirmed euploid, were aggregated with CD1 morulae. Chimeric males were crossed with WT Institute for Cancer Research (ICR) females. Germline transmission was confirmed for the line H1-2. *Nkx2-1*^{mCherry} mouse line was maintained in a mixed 129 × ICR genetic

(C) Images of colonies isolated in assay described in (B). Primary (1^{ary}), secondary (2^{ary}), and tertiary (3^{ary}) colonies are 18 (p.1), 23 (p.2), and 22 days old (p.3), respectively. The number of daughter colonies is indicated in parentheses.
(D) Quantitative real-time PCR with RNA isolated from colonies depicted in (C) from three serial series, as well as the initial sorted E12.5 mC^+ proximal (prox.) cells and nonsorted (n.-s.) adult proximal tissue control. ΔCt heatmap is shown with normalization of Ct values of indicated target genes to *Actb* (ΔCt). The cutoff was set to a ΔCt of 8 (Ct 24.5–36.9 for *Actb*).
See also Table S2.

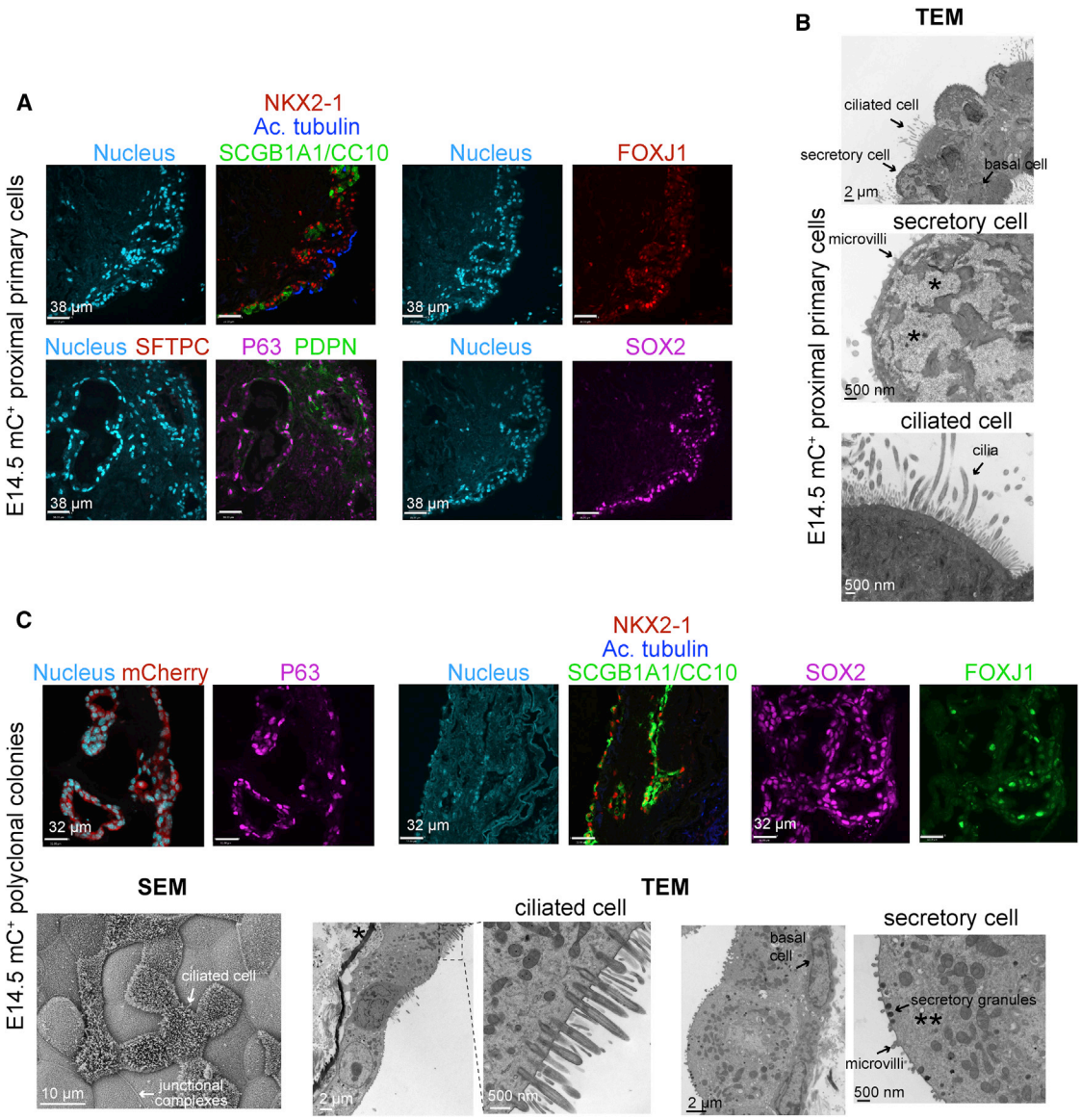

Figure 6. Repopulation of Decellularized Lung Scaffolds with E14.5 Primary or Polyclonal Cultured Cells

(A) Immunostaining of scaffolds repopulated with primary E14.5 *Nkx2-1*-mC$^+$ cells freshly sorted from proximal lungs.

(B) TEM showing secretory, ciliated, and basal cells in addition to epithelial polarization. Asterisk (*) indicates glycogen lakes.

(C) Immunostaining (top) and electron microscopy (bottom) of scaffolds repopulated with polyclonal E14.5 mC$^+$ cultured cells. The single asterisk (*) indicates that the matrix is representative of compact electron opaque and loosely associated filamentous material. The double asterisks (**) indicate that the cytoplasm contains endoplasmic reticulum- and Golgi-derived membranes typical of a secretory cell. See also Figures S6 and S7 and Tables S1 and S3.

background. Refer to the Supplemental Experimental Procedures for genotyping.

Mouse Husbandry

Mouse husbandry and manipulations were done in agreement with Canadian Council for Animal Care guidelines at the Toronto Centre for Phenogenomics. The day of the vaginal plug was considered as E0.5.

Flow Cytometry

Fetal tissues were microdissected with tweezers under a stereomicroscope. The trachea and two primary extrapulmonary bronchi (i.e., proximal lung region) were separated from the branching distal lung region (Figure 1B). Tissue pools were trypsinized at 37°C (0.25% trypsin-EDTA; Invitrogen). For E16.5 and older distal lungs, red blood cells were lysed with a commercial buffer (Sigma-Aldrich). Cells were resuspended at $\leq 5 \times 10^6$/ml in 1% FBS-PBS

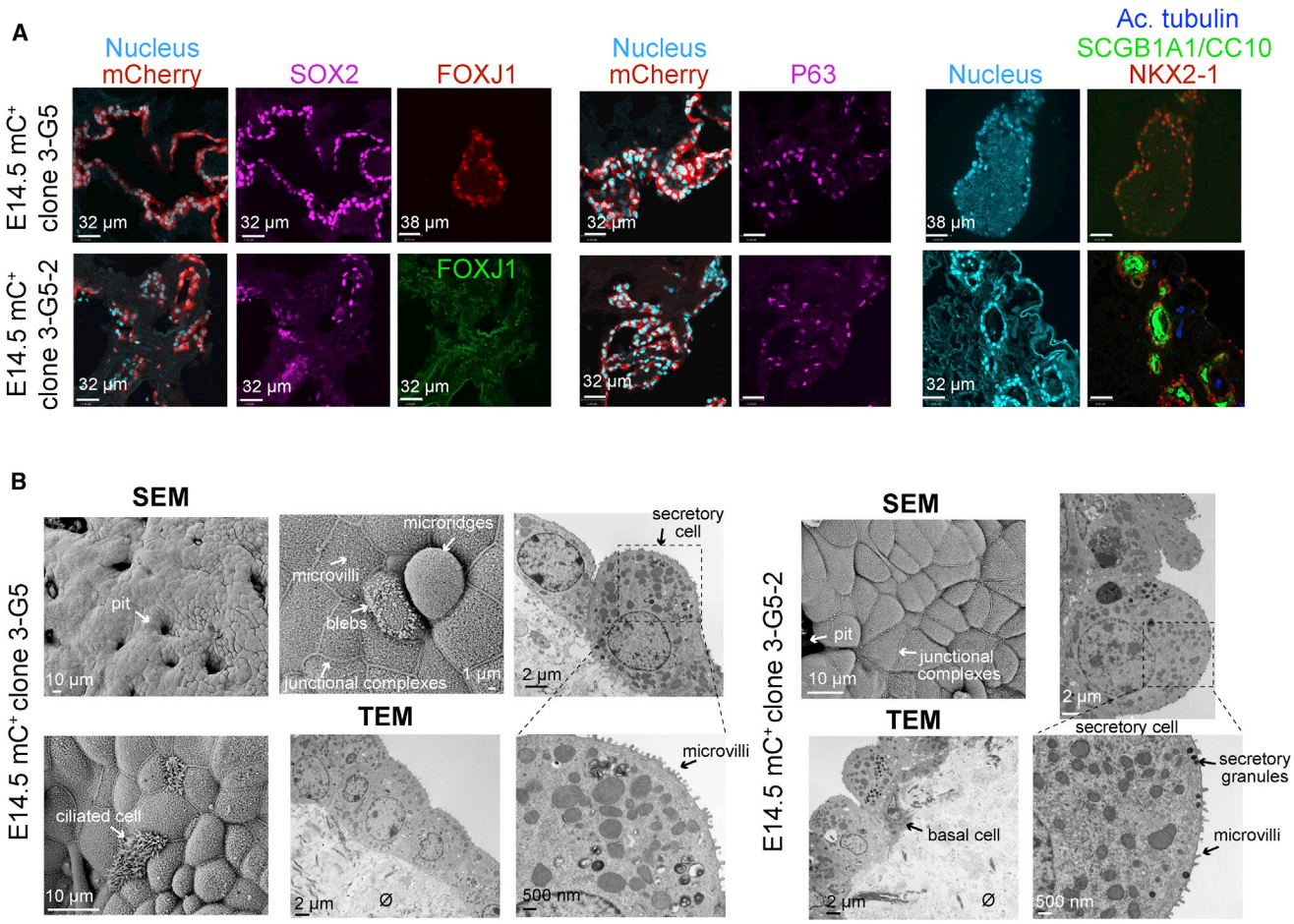

Figure 7. Repopulation of Decellularized Lung Scaffolds with Serial Clonal Cultures Derived from E14.5 Proximal Lungs

(A) Section immunostaining of scaffolds repopulated with indicated *Nkx2-1*-mC$^+$ clonal cultures.

(B) SEM and TEM showing the epithelial morphology of clonal cultures in scaffolds. Overall, clonal cultures give rise to at least two to three distinct proximal cell types. Ø, decellularized lung matrix.

See also Figures S6 and S7 and Tables S1 and S3.

with propidium iodide to exclude dead cells (Sigma-Aldrich; P4864, 1:3,000) and sorted with a MoFlo (Beckman Coulter) apparatus. For cell-mixing experiments, E14.5 proximal lung cells were sorted either from the *Nkx2-1*^{mCherry} mouse line (mCherry expression) or EGFP mice (B5/EGFP: STOCK Tg(CMV-GFP) 1Nagy) (EpCAM-PECy7 staining; Table S3) (Hadjantonakis et al., 1998). For staining protocols, refer to the Supplemental Experimental Procedures. Results were analyzed with FACSDiva (BD Biosciences) and FlowJo (TreeStar) software.

Culture of Primary Colonies

Control media 1 (Figure S3A) was prepared with the following reagents: Dulbecco's modified Eagle's medium/F12 (Invitrogen), 3% FBS (Invitrogen), 10 µg/ml insulin (Sigma-Aldrich), 10 µM forskolin (Sigma-Aldrich), 10 µM IBMX (Sigma-Aldrich), 25 ng/ml EGF (R&D Systems), 10 ng/ml HGF (R&D Systems), 25 ng/ml FGF7 (R&D Systems), 100 ng/ml FGF1 (R&D Systems), 30 ng/ml FGF10 (R&D Systems), 100 U/ml penicillin/streptomycin (Invitrogen), 2 mM GlutaMAX (Invitrogen), and 0.15 mM α-thioglycerol (Sigma-Aldrich). Medium was mixed 1:1 with growth factor-reduced Matrigel (BD Biosciences; #356231) and solidified in inserts (0.4 µm pores; BD Biosciences; #353180 and #353095). Liquid media were added to the bottom chamber and changed every 2–3 days. Cells were maintained at 37°C with 10% CO_2. Additional details are included in the Supplemental Experimental Procedures.

Fluorescence Imaging

Macroscopic imaging of tissues or fetuses was done with a stereomicroscope (Leica MZ16F). Imaging of colonies was done with the stereomicroscope or a Leica DMI6000B inverted microscope. Both systems are described in the Supplemental Experimental Procedures.

Quantitative Real-Time PCR

RNA was extracted with TRIzol (Ambion), and cDNA was synthesized with the QuantiTect Kit (QIAGEN). Gene expression was

assessed using the Roche LightCycler 480 with custom SYBR Green assays described in Table S2 and the Supplemental Experimental Procedures. Threshold cycle (Ct) values were determined using the advanced relative quantification algorithm for each target gene (Ct_{target}) as well as *Actb* and *Hprt1* reference genes ($Ct_{reference}$). ΔCt heatmaps (i.e., $\Delta Ct = Ct_{target} - \text{average } Ct_{reference}$) were produced in part using MeV, with or without the hierarchical clustering function (Saeed et al., 2006). The comparative Ct method was employed ($2^{-\Delta\Delta Ct}$; $\Delta\Delta Ct = \Delta Ct_{sample} - \Delta Ct_{calibrator}$) for Figures S3D–S3L, S4B–S4H, and S5E. Relative gene expression values for calibrators were set to one (1), and values of target genes were represented as fold changes.

Repopulation of Decellularized Rat Lung Scaffolds

Optimized procedures to decellularize the distal lungs of rats were adapted from previously published protocols by Petersen et al. (2010) and will be described elsewhere (S.S. and M.P., unpublished data). Dissociated primary and cultured cells, 50,000–100,000 cells or 10–20 colonies, were seeded onto 300- to 400-μm-thick sections of decellularized scaffolds. Cultures were maintained for 14–21 days on floating membranes (Nuclepore Track-Etched membranes, 8.0 μm pores) in a serum-free basal differentiation medium changed every other day (S.S. and M.P., unpublished data). Cultures were maintained at 37°C with 5% CO_2.

Histology and Immunostaining

For cryosections, samples were fixed with 4% formaldehyde, incubated in 30% sucrose, embedded in optimum cutting temperature compound (Tissue-Tek), and sectioned at 10 μM. For paraffin sections, primary tissues were fixed as described above, dehydrated, and embedded in paraffin wax. Colonies or lung scaffolds were embedded in HistoGel (Thermo Scientific) prior to fixation. Samples were processed according to standard conditions and sectioned at 4 μM. Standard immunostaining techniques and confocal microscopy are described in the Supplemental Experimental Procedures. Antibodies are listed in Table S3.

Electron Microscopy

Cell cultures were fixed in 2.5% glutaraldehyde in 0.1 M phosphate buffer (pH 7.4). Details for TEM and SEM are described in the Supplemental Experimental Procedures.

SUPPLEMENTAL INFORMATION

Supplemental Information includes Supplemental Experimental Procedures, seven figures, and three tables and can be found with this article online at http://dx.doi.org/10.1016/j.stemcr.2014.07.010.

ACKNOWLEDGMENTS

We thank Jorge Cabezas, Jodi Garner, and Sukhmani Sethi for technical support as well as Dr. Nadeem Moghal for helpful discussion. We are grateful to Jorge Cabezas, Monica Pereira, Sandra Tondat, Suzanne MacMaster, and Marina Gertsenstein at the Transgenic Facility of the Toronto Centre for Phenogenomics (TCP). We acknowledge Dr. Sheyun Zhao, Pier Andrée Penttilä, and Dr. Julie Yuan at the SickKids-UHN Flow Cytometry Facility as well as Lily Morikawa and Patricia Feugas at the TCP histology core. We thank Michael Woodside and Paul Paroutis at the SickKids Imaging Facility. The pFlexible plasmid was a gift from Dr. Allan Bradley. This research was supported by a grant from the Canadian Institutes of Health Research (CIHR; grant RMF-92088). M.B. received fellowships from a CIHR/Canadian Lung Association/GlaxoSmithKline partnership and from the Fonds de la Recherche en Santé du Québec.

Received: December 4, 2013
Revised: July 22, 2014
Accepted: July 24, 2014
Published: September 4, 2014

REFERENCES

Alanis, D.M., Chang, D.R., Akiyama, H., Krasnow, M.A., and Chen, J. (2014). Two nested developmental waves demarcate a compartment boundary in the mouse lung. Nat. Commun. *5*, 3923.

Broers, J.L., de Leij, L., Rot, M.K., ter Haar, A., Lane, E.B., Leigh, I.M., Wagenaar, S.S., Vooijs, G.P., and Ramaekers, F.C. (1989). Expression of intermediate filament proteins in fetal and adult human lung tissues. Differentiation *40*, 119–128.

Chang, D.R., Martinez Alanis, D., Miller, R.K., Ji, H., Akiyama, H., McCrea, P.D., and Chen, J. (2013). Lung epithelial branching program antagonizes alveolar differentiation. Proc. Natl. Acad. Sci. USA *110*, 18042–18051.

Daniely, Y., Liao, G., Dixon, D., Linnoila, R.I., Lori, A., Randell, S.H., Oren, M., and Jetten, A.M. (2004). Critical role of p63 in the development of a normal esophageal and tracheobronchial epithelium. Am. J. Physiol. Cell Physiol. *287*, C171–C181.

Delplanque, A., Coraux, C., Tirouvanziam, R., Khazaal, I., Puchelle, E., Ambros, P., Gaillard, D., and Péault, B. (2000). Epithelial stem cell-mediated development of the human respiratory mucosa in SCID mice. J. Cell Sci. *113*, 767–778.

Desai, T.J., Brownfield, D.G., and Krasnow, M.A. (2014). Alveolar progenitor and stem cells in lung development, renewal and cancer. Nature *507*, 190–194.

El-Gawad, M.A., and Westfall, J.A. (2000). Comparative ultrastructure of Clara cells in neonatal and older cattle. J. Morphol. *244*, 143–151.

Engelhardt, J.F., Schlossberg, H., Yankaskas, J.R., and Dudus, L. (1995). Progenitor cells of the adult human airway involved in submucosal gland development. Development *121*, 2031–2046.

Guha, A., Vasconcelos, M., Cai, Y., Yoneda, M., Hinds, A., Qian, J., Li, G., Dickel, L., Johnson, J.E., Kimura, S., et al. (2012). Neuroepithelial body microenvironment is a niche for a distinct subset of Clara-like precursors in the developing airways. Proc. Natl. Acad. Sci. USA *109*, 12592–12597.

Guha, A., Vasconcelos, M., Zhao, R., Gower, A.C., Rajagopal, J., and Cardoso, W.V. (2014). Analysis of Notch signaling-dependent gene expression in developing airways reveals diversity of Clara cells. PLoS One *9*, e88848.

Hadjantonakis, A.K., Gertsenstein, M., Ikawa, M., Okabe, M., and Nagy, A. (1998). Generating green fluorescent mice by germline transmission of green fluorescent ES cells. Mech. Dev. *76*, 79–90.

Hegab, A.E., Ha, V.L., Gilbert, J.L., Zhang, K.X., Malkoski, S.P., Chon, A.T., Darmawan, D.O., Bisht, B., Ooi, A.T., Pellegrini, M., et al. (2011). Novel stem/progenitor cell population from murine tracheal submucosal gland ducts with multipotent regenerative potential. Stem Cells *29*, 1283–1293.

Kimura, J., and Deutsch, G.H. (2007). Key mechanisms of early lung development. Pediatr. Dev. Pathol. *10*, 335–347.

Kimura, S., Hara, Y., Pineau, T., Fernandez-Salguero, P., Fox, C.H., Ward, J.M., and Gonzalez, F.J. (1996). The T/ebp null mouse: thyroid-specific enhancer-binding protein is essential for the organogenesis of the thyroid, lung, ventral forebrain, and pituitary. Genes Dev. *10*, 60–69.

Lazzaro, D., Price, M., de Felice, M., and Di Lauro, R. (1991). The transcription factor TTF-1 is expressed at the onset of thyroid and lung morphogenesis and in restricted regions of the foetal brain. Development *113*, 1093–1104.

Li, Y., and Linnoila, R.I. (2012). Multidirectional differentiation of Achaete-Scute homologue-1-defined progenitors in lung development and injury repair. Am. J. Respir. Cell Mol. Biol. *47*, 768–775.

Longmire, T.A., Ikonomou, L., Hawkins, F., Christodoulou, C., Cao, Y., Jean, J.C., Kwok, L.W., Mou, H., Rajagopal, J., Shen, S.S., et al. (2012). Efficient derivation of purified lung and thyroid progenitors from embryonic stem cells. Cell Stem Cell *10*, 398–411.

Massaro, G.D., Davis, L., and Massaro, D. (1984). Postnatal development of the bronchiolar Clara cell in rats. Am. J. Physiol. *247*, C197–C203.

McQualter, J.L., Yuen, K., Williams, B., and Bertoncello, I. (2010). Evidence of an epithelial stem/progenitor cell hierarchy in the adult mouse lung. Proc. Natl. Acad. Sci. USA *107*, 1414–1419.

Minoo, P., Su, G., Drum, H., Bringas, P., and Kimura, S. (1999). Defects in tracheoesophageal and lung morphogenesis in Nkx2.1(-/-) mouse embryos. Dev. Biol. *209*, 60–71.

Nagy, A., Rossant, J., Nagy, R., Abramow-Newerly, W., and Roder, J.C. (1993). Derivation of completely cell culture-derived mice from early-passage embryonic stem cells. Proc. Natl. Acad. Sci. USA *90*, 8424–8428.

Péault, B., Tirouvanziam, R., Sombardier, M.N., Chen, S., Perricaudet, M., and Gaillard, D. (1994). Gene transfer to human fetal pulmonary tissue developed in immunodeficient SCID mice. Hum. Gene Ther. *5*, 1131–1137.

Perl, A.K., Wert, S.E., Nagy, A., Lobe, C.G., and Whitsett, J.A. (2002). Early restriction of peripheral and proximal cell lineages during formation of the lung. Proc. Natl. Acad. Sci. USA *99*, 10482–10487.

Petersen, T.H., Calle, E.A., Zhao, L., Lee, E.J., Gui, L., Raredon, M.B., Gavrilov, K., Yi, T., Zhuang, Z.W., Breuer, C., et al. (2010). Tissue-engineered lungs for in vivo implantation. Science *329*, 538–541.

Pohlenz, J., Dumitrescu, A., Zundel, D., Martiné, U., Schönberger, W., Koo, E., Weiss, R.E., Cohen, R.N., Kimura, S., and Refetoff, S. (2002). Partial deficiency of thyroid transcription factor 1 produces predominantly neurological defects in humans and mice. J. Clin. Invest. *109*, 469–473.

Que, J., Okubo, T., Goldenring, J.R., Nam, K.T., Kurotani, R., Morrisey, E.E., Taranova, O., Pevny, L.H., and Hogan, B.L. (2007). Multiple dose-dependent roles for Sox2 in the patterning and differentiation of anterior foregut endoderm. Development *134*, 2521–2531.

Que, J., Luo, X., Schwartz, R.J., and Hogan, B.L. (2009). Multiple roles for Sox2 in the developing and adult mouse trachea. Development *136*, 1899–1907.

Rawlins, E.L., Ostrowski, L.E., Randell, S.H., and Hogan, B.L. (2007). Lung development and repair: contribution of the ciliated lineage. Proc. Natl. Acad. Sci. USA *104*, 410–417.

Rawlins, E.L., Clark, C.P., Xue, Y., and Hogan, B.L. (2009a). The Id2+ distal tip lung epithelium contains individual multipotent embryonic progenitor cells. Development *136*, 3741–3745.

Rawlins, E.L., Okubo, T., Xue, Y., Brass, D.M., Auten, R.L., Hasegawa, H., Wang, F., and Hogan, B.L. (2009b). The role of Scgb1a1+ Clara cells in the long-term maintenance and repair of lung airway, but not alveolar, epithelium. Cell Stem Cell *4*, 525–534.

Raymond, C.S., and Soriano, P. (2007). High-efficiency FLP and PhiC31 site-specific recombination in mammalian cells. PLoS One *2*, e162.

Rock, J.R., Onaitis, M.W., Rawlins, E.L., Lu, Y., Clark, C.P., Xue, Y., Randell, S.H., and Hogan, B.L. (2009). Basal cells as stem cells of the mouse trachea and human airway epithelium. Proc. Natl. Acad. Sci. USA *106*, 12771–12775.

Saeed, A.I., Bhagabati, N.K., Braisted, J.C., Liang, W., Sharov, V., Howe, E.A., Li, J., Thiagarajan, M., White, J.A., and Quackenbush, J. (2006). TM4 microarray software suite. Methods Enzymol. *411*, 134–193.

Shannon, J.M., Gebb, S.A., and Nielsen, L.D. (1999). Induction of alveolar type II cell differentiation in embryonic tracheal epithelium in mesenchyme-free culture. Development *126*, 1675–1688.

Smolich, J.J., Stratford, B.F., Maloney, J.E., and Ritchie, B.C. (1978). New features in the development of the submucosal gland of the respiratory tract. J. Anat. *127*, 223–238.

Song, H., Yao, E., Lin, C., Gacayan, R., Chen, M.H., and Chuang, P.T. (2012). Functional characterization of pulmonary neuroendocrine cells in lung development, injury, and tumorigenesis. Proc. Natl. Acad. Sci. USA *109*, 17531–17536.

Tata, P.R., Mou, H., Pardo-Saganta, A., Zhao, R., Prabhu, M., Law, B.M., Vinarsky, V., Cho, J.L., Breton, S., Sahay, A., et al. (2013). Dedifferentiation of committed epithelial cells into stem cells in vivo. Nature *503*, 218–223.

Treutlein, B., Brownfield, D.G., Wu, A.R., Neff, N.F., Mantalas, G.L., Espinoza, F.H., Desai, T.J., Krasnow, M.A., and Quake, S.R. (2014). Reconstructing lineage hierarchies of the distal lung epithelium using single-cell RNA-seq. Nature *509*, 371–375.

van der Weyden, L., Adams, D.J., Harris, L.W., Tannahill, D., Arends, M.J., and Bradley, A. (2005). Null and conditional semaphorin 3B alleles using a flexible puroDeltatk loxP/FRT vector. Genesis *41*, 171–178.

Wansleeben, C., Barkauskas, C.E., Rock, J.R., and Hogan, B.L.M. (2013). Stem cells of the adult lung: their development and role in homeostasis, regeneration, and disease. Wiley Interdiscip Rev Dev Biol *2*, 131–148.

Wansleeben, C., Bowie, E., Hotten, D.F., Yu, Y.R., and Hogan, B.L. (2014). Age-related changes in the cellular composition and epithelial organization of the mouse trachea. PLoS One *9*, e93496.